Slovenian **Medical** Journal

Regenerative potential of platelet-rich plasma as an adjuvant to scaffolds in the repair of critical bone tissue defects

Regenerativni potencial plazme, bogate s trombociti, kot dodatka k opornim strukturam pri popravljanju kritičnih okvar kostnega tkiva

Grigory Demyashkin, Matvey Vadyukhin, Evgenia Samborskaya, Alexandr Kravets, Irina Ignatko, Vera Rostovskaya

Abstract

Background: A critical-size bone defect is defined as damage that exceeds the body's intrinsic regenerative capacity for repair. The restoration of critical-size bone defects remains a major challenge in regenerative medicine and tissue engineering. Recent research emphasizes the importance of combining structural scaffolds with cellular and biologically active components to enhance bone regeneration. Objective: to develop and evaluate the structural and functional effects on bone repair and neoangiogenesis of a collagen-based scaffold implanted into a critical-size bone defect with platelet-rich plasma (PRP) in combination with stromal vascular fraction (SVF) cells.

Methods: Forty Wistar rats were divided into groups: Group I (n = 10) received a collagen sponge (CS); Group II (n = 15) received a CS + SVF; Group III (n = 15) received a CS/SVF scaffold + PRP. Foreign material was received locally at the site of a critical-size bone defect. Micro-CT, haematological (clinical blood analyses), and histological (haematoxylin and eosin staining) analyses were performed. All animals were euthanized three months after implantation.

Results: Micro-CT and histological evaluation revealed enhanced scaffold osteointegration, increased bone formation, and vascularisation in the CS+SVF+PRP group compared to controls. PRP significantly improved bone volume, surface area, and material density in the defect zone. Histological scoring confirmed more pronounced osteogenesis and neovascularisation in experimental groups. Haematological data indicated increased hemoglobin without signs of systemic inflammation. Local inflammatory response was minimal in the PRP group.

Conclusion: The combination of collagen matrix, SVF, and PRP exhibits high biocompatibility and pronounced regenerative potential, providing a synergistic effect that promotes osteogenesis and angiogenesis. This approach shows promise for future applications in bone tissue engineering and warrants further molecular-level investigation.

I.M. Sechenov First Moscow State Medical University (Sechenov University), Moscow, Russia

Correspondence / Korespondenca: Matvey Vadyukhin, e: vma20@mail.ru

Keywords: neovascularization; bone regeneration; tomography; biocompatible materials; growth factors

Ključne besede: neovaskularizacija; regeneracija kosti; tomografija; biokompatibilni materiali; rastni faktorji

Received / Prispelo: 27. 5. 2025 | **Accepted / Sprejeto:** 25. 7. 2025

Cite as / Citirajte kot: Demyashkin G, Vadyukhin M, Samborskaya E, Kravets A, Ignatko I, Rostovskaya V. Regenerative potential of platelet-rich plasma as an adjuvant to scaffolds in the repair of critical bone tissue defects. Zdrav Vestn. 2025;94(7–8):178–85. **DOI:** https://doi.org/10.6016/ZdravVestn.3636

Izvleček

Izhodišče: Kritična kostna poškodba je opredeljena kot poškodba, ki presega lastno regenerativno sposobnost telesa za popravilo. Obnova kritičnih kostnih poškodb predstavlja velik izziv v regenerativni medicini in tkivnem inženiringu. Nedavne raziskave poudarjajo pomen kombiniranja opornih struktur s celičnimi in biološko aktivnimi komponentami za izboljšanje regeneracije kosti. Cilj: razviti in ovrednotiti strukturne in funkcionalne učinke na popravilo kosti in neoangiogenezo kolagenske opore, vsajene v kritično kostno poškodbo s plazmo, bogato s trombociti (PRP), v kombinaciji s stromalnimi vaskularnimi frakcijskimi (SVF) celicami.

Metode: Štirideset Wistar podgan je bilo razdeljenih v tri skupine: skupina I (n = 10) je prejela kolagensko gobo (CS), skupina II (n = 15) CS + SVF, skupina III (n = 15) pa je prejela CS/SVF ogrodje + PRP. Tuj material je bil lokalno vstavljen na mestu kritične kostne poškodbe. Izvedene so bile mikro-CT, hematološke (klinične krvne analize) in histološke (barvanje s hematoksilinom in eozinom) analize. Vse živali so bile tri mesece po implantaciji evtanazirane.

Rezultati: Mikro-CT in histološka ocena sta pokazali izboljšano osteointegracijo ogrodja, povečano tvorbo kosti in vaskularizacijo v skupini CS+SVF+PRP v primerjavi s kontrolno skupino. PRP je znatno izboljšala kostni volumen, površino in gostoto materiala v področju okvare. Histološka ocena je potrdila izrazitejšo osteogenezo in neovaskularizacijo pri eksperimentalnih skupinah. Hematološki podatki so pokazali povečano raven hemoglobina brez znakov sistemskega vnetja. Lokalni vnetni odziv je bil v skupini PRP minimalen.

Zaključek: Kombinacija kolagenske osnove, SVF in PRP kaže visoko biokompatibilnost in izrazit regenerativni potencial, kar zagotavlja sinergistični učinek, ki spodbuja osteogenezo in angiogenezo. Ta pristop je obetaven za prihodnje aplikacije v tkivnem inženiringu kosti in upravičuje nadaljnje raziskave na molekularni ravni.

1 Introduction

The restoration of bone tissue in cases of critical-size bone defects (CSBD) remains one of the key challenges in modern regenerative medicine, traumatology, and maxillofacial surgery (1). When the extent of damage exceeds the body's intrinsic regenerative capacity for repair (based on the current definition of CSBD), the use of biomaterials capable of stimulating osteogenesis, neoangiogenesis, and bone tissue remodelling becomes essential (2,3). In this context, significant attention is being directed toward the development and optimization of strategies aimed at enhancing the repair of bone defects.

Currently, a wide range of materials is employed in both experimental and clinical settings, including natural and synthetic polymers, calcium-based ceramics (such as hydroxyapatite and β-tricalcium phosphate), bioactive glass, and various composite materials (4-6). In parallel, cell-based technologies, particularly the use of mesenchymal stem cells (MSCs) with osteogenic differentiation potential, are being actively introduced into regenerative approaches (7). However, despite their proven biocompatibility and osteoconductive properties, these materials present several limitations, including the brittleness and low resorbability of ceramics, the suboptimal mechanical strength of polymers, and technical difficulties associated with the isolation and cultivation of cellular components (8).

Despite significant progress in the field, no implantable material currently available fully meets all the criteria required for the effective restoration of critical-size bone defects (9), which highlights the need for further research aimed at evaluating the effectiveness of novel biocomposites and their potential combinations. In particular, the development of multifunctional scaffolds that integrate the advantages of various components appears to be a promising strategy for accelerating osteogenesis and improving the structural and morphological characteristics of newly formed bone tissue.

In recent years, a particularly auspicious direction has been the design of composite bioconstructs that incorporate structural, cellular, and biologically active elements within a single system (10). One such approach involves the implantation of composite scaffolds comprising a collagen-based matrix (collagen sponge, CS), stromal vascular fraction (SVF) derived from adipose tissue, and platelet-rich plasma (PRP). The collagen matrix provides three-dimensional support and directed osteoconduction; the cellular fraction serves as a source of osteogenic and angiogenic progenitors; and PRP delivers a broad spectrum of growth factors that enhance regenerative processes (11-14).

Thus, combinations of PRP+SVF or Collagen+PRP or Collagen+SVF have already been studied by other authors (15). We offer a multicomponent scaffold, which is a self-sufficient regenerative material with all the necessary properties for effective reparation. At the same time, it may have high biocompatibility, and the combination of "collagen matrix+PRP+SVF" has not yet been described in the scientific literature. Moreover, each component plays its specific role: collagen – framework and strength, PRP – source of regenerative and pro-angiogenic factors, SVF – substrate cells with the ability to proliferate and differentiate in the osteogenic direction.

The objective of the study was to develop and evaluate the structural and functional effects on bone repair and neoangiogenesis of a collagen-based scaffold implanted into a critical-size bone defect with platelet-rich plasma (PRP) in combination with stromal vascular fraction (SVF) cells.

2 Methods

Experimental animals (Wistar rats; n = 40; body weight 220–240 g) were randomly assigned to three groups according to the study design using power analysis:

- Group I (n = 10) – control group: a collagen sponge (CS) was implanted into the critical-size bone defect site;
- Group II (n = 15) – experimental group: a scaffold composed of a collagen matrix and stromal vascular fraction (SVF) cells was implanted into the defect site (CS+SVF);
- Group III (n = 15) – experimental group: a composite scaffold consisting of a collagen matrix and SVF cells was implanted in combination with local application of autologous platelet-rich plasma-derived growth factors (CS+SVF+PRP).

All animals were euthanized three months after surgery by administering high doses of a combined anaesthetic (ketamine + xylazine). All procedures were carried out in compliance with ethical standards and regulatory guidelines for the humane treatment of laboratory animals, including the Declaration of Helsinki (WMA, 1964), the decision of the Eurasian Economic Commission Council dated 16 May 2016, No. 38 "On Approval of the Rules for Conducting Studies to Assess the Biological Effects of Medical Devices," Directive 2010/63/EU of the European Parliament and of the Council of 22 September 2010 on the protection of animals used for scientific purposes.

2.1 Surgical procedure

For the surgical procedure, each rat was placed in the prone position on the operating table and had its limbs secured. Following preoperative preparation, which included intramuscular administration of gentamicin (0.1 ml/kg), anesthesia was induced with an intramuscular injection of Zoletil (20.0 mg/kg) and Rometar (5 mg/kg). The frontal region of the head was shaved and treated with an antiseptic solution. A midline skin incision approximately 1.5 cm in length was made in the caudal direction, and retractors were applied to expose the cranial surface. The overlying soft tissues and periosteum were gently detached at the site of the planned osteotomy. A craniotomy was performed using a manual surgical drill, creating a critical-size bone defect (0.7–1.0 cm in diameter). The defect area was thoroughly cleaned of bone debris and blood, and the integrity of the dura mater and underlying brain structures was verified. A scaffold corresponding to the size of the trepanation window was implanted into the defect. The composition of the scaffold was selected according to the experimental group design. Soft tissues were closed with a continuous suture using Vycril 2/0, and the skin was closed with interrupted sutures using Vycril Rapid 3/0. The surgical site was treated with an antiseptic solution postoperatively.

2.2 Isolation and preparation of Stromal Vascular Fraction (SVF)

Adipose tissue harvesting was performed under general anaesthesia (xylazine 10 mg/kg + ketamine 80 mg/kg, intramuscularly) under aseptic conditions. Subcutaneous adipose tissue from the inguinal region was used as the source of cellular material. The harvested tissue was washed three times in sterile phosphate-buffered saline (PBS) supplemented with antibiotics (penicillin 100 U/ml, streptomycin 100 μg/ml) and mechanically minced. Enzymatic digestion was carried out at 37 °C for 30 minutes using collagenase type I solution (0.075% in PBS). Following incubation, enzymatic activity was neutralized by adding Dulbecco's Modified Eagle Medium (DMEM) supplemented with 10% fetal bovine serum (FBS). The resulting cell suspension was filtered through a 100 μm nylon mesh and centrifuged at 1200 rpm for 10 minutes. The floating adipose layer was removed, and the pellet containing SVF cells was resuspended in sterile 0.9% NaCl solution. The obtained cell suspension was standardized to a volume of 50 μl, containing approximately 1×10^6 cells, and was used to saturate the collagen scaffold immediately before implantation in Groups II and III.

2.3 Platelet-Rich Plasma (PRP) preparation

Autologous leukocyte-poor platelet-rich plasma (LP-PRP) was obtained by collecting 1.5–2.0 ml of peripheral blood from the tail vein of rats using heparinised syringes (sodium heparin, 10 U/ml) under aseptic conditions. The collected blood was processed using a two-step centrifugation protocol. The first centrifugation was performed at 400 g for 10 minutes at room temperature to separate the plasma layer containing platelets and a minimal number of leukocytes. This supernatant was transferred to a clean tube and subjected to a second centrifugation at 800 g for 10 minutes to pellet the platelets. The upper fraction of platelet-poor plasma was discarded, and the remaining 0.3–0.5 ml was gently resuspended to obtain LP-PRP. Prior to application, the PRP was activated by adding 10% calcium chloride solution (10 µl per 100 µl of PRP) and incubated for 10 minutes at 37 °C. The activated PRP (30–50 µl) was then applied onto the collagen scaffold pre-seeded with stromal vascular fraction cells, as used in Group III.

2.4 Haematological analysis

Blood samples were collected from the auricular vein in compliance with the standard operating procedure "Blood Collection in Laboratory Animals" using tubes containing 3.8% sodium citrate solution (50 µl). For analysis, 0.5 ml of whole blood was used. Standard haematological parameters were measured using a haematology analyzer (Hemalite 1280, Dixion, Russia).

2.5 Micro-Computed Tomography (Micro-CT)

Prepared cranial specimens were visualized using a Bruker Skyscan 1276 X-ray microtomograph (Bruker, Belgium). The assessment included evaluation of scaffold positioning and peripheral bone ingrowth, specifically the penetration of newly formed bone structures into the critical-size defect zone. The following morphometric parameters were analyzed by micro-CT: tissue volume within the defect zone (mm^3), tissue surface area within the defect (mm^2), and surface density of the material (mm^2).

2.6 Histological examination

For histological analysis, cranial specimens containing the defect area were fixed in 10% neutral buffered formalin, dehydrated, decalcified, processed in a tissue processor, embedded in paraffin blocks, and sectioned at a thickness of 3 µm. The sections were stained with haematoxylin and eosin (H&E). Histological slides were examined using a Leica DM2000 light microscope with microphotography capabilities.

The following morphological parameters were evaluated using a semi-quantitative scoring system: on the side of the implant – degree of implant resorption, formation of woven or lamellar bone tissue, cellular inflammatory infiltration (lymphocytes, plasma cells, and cells of the monocyte–macrophage lineage), and degree of exudative inflammation; on the host tissue side – neovascularisation within the implantation bed, fibrosis, and necrosis. Scoring criteria were as follows:

1. Implant resorption and bone tissue formation:
   - 1 point – mild;
   - 2 points – moderate;
   - 3 points – extensive.
2. Inflammatory infiltration (assessed at ×400 magnification by counting immune cells per field of view):
   - 1 point – 0–5 cells;
   - 2 points – 6–10 cells;
   - 3 points – more than 10 cells (dense inflammatory infiltrate).
3. Neovascularisation (assessed by the number of capillary proliferation foci):
   - 1 point – 0–3 foci;
   - 2 points – 4–7 capillaries with associated fibroblasts;
   - 3 points – more than 7 capillaries with abundant fibroblastic proliferation.
4. Fibrosis:
   - 1 point – absent;
   - 2 points – narrow band of fibrous connective tissue;
   - 3 points – wide band of dense fibrous tissue (scar formation).
5. Necrosis in the peri-implant zone: 0 points – absent; 1 point – focal necrosis of surrounding tissues.

2.7 Statistical analysis

The data obtained from quantitative assessments were processed using the SPSS 12 for Windows statistical software package (IBM Analytics, USA). Results are presented as mean ± standard deviation (M ± SD). Group comparisons were performed using one-way analysis of variance (ANOVA). Additionally, nonparametric statistical tests were applied, including the Kruskal–Wallis test and the Mann–Whitney U test. A p-value of less than 0.05 was considered statistically significant.

The study design was approved by the Local Ethics Committee of I.M. Sechenov First Moscow State Medical University (protocol №148 from 12/11/23).

3 Results

In the group receiving the scaffold composed of collagen, stromal vascular fraction, and platelet-rich plasma (CS+SVF+PRP), blood analysis revealed elevated levels of haemoglobin, haematocrit, platelet count, and plateletcrit compared to both the control group and the group implanted with the scaffold without additional PRP administration. No statistically significant differences in hematological parameters were observed between the CS+SVF+PRP and the CS+SVF groups. No increase in markers of systemic inflammatory response was observed in any of the blood samples (Table 1).

Micro-computed tomography of cranial sections in all groups revealed inward growth of bone structures into the implantation site, with the most pronounced ingrowth observed in the group treated with the CS+SVF+PRP scaffold (Figure 1). Quantitative analysis demonstrated an increase in both the volume and surface area of newly formed bone tissue in the implantation zone following additional PRP application. Moreover, an increase in surface density was noted, indicating improved qualitative characteristics of the regenerated bone tissue (Table 2).

These findings were further supported by histological analysis, which confirmed varying degrees of osteo-histogenesis and neovascularisation. In the control group, histological examination revealed limited replacement of the biodegradable scaffold (approximately one-quarter of the defect area) by newly formed bone. Reticulated-trabecular structures containing osteogenic cells, primarily osteoclasts, were observed, surrounded by fibrous connective tissue with blood vessels, indicating a mild degree of osteogenesis and moderate neovascularisation. A moderate foreign-body inflammatory response was detected in the peri-implant area, represented mainly by mononuclear cell infiltration of lymphoid-histiocytic origin.

Similar patterns were observed in Groups II and III, although the extent of scaffold replacement was greater – one-third and two-fifths of the defect area, respectively. The degree of osteogenesis in these groups was evaluated as moderate and pronounced. Inflammatory infiltration in the peri-implant area was less prominent compared to the control group and was limited to scattered lymphoid-histiocytic cells. Additionally, neovascular proliferation was more pronounced in the CS+SVF+PRP group. Notably, no signs of fibrosis or necrosis were observed in the implantation area in any of the studied groups (Table 3, Figure 1).

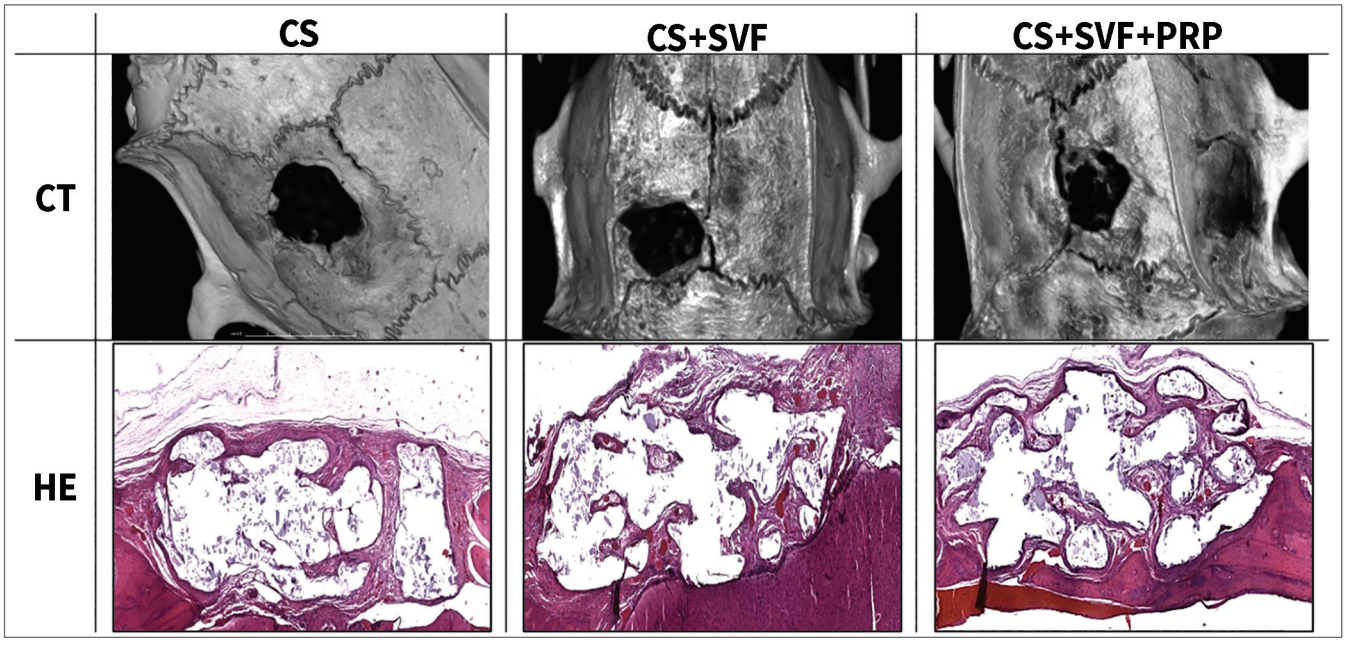

Figure 1: Cranial specimens from the control (CS) and experimental groups (CS+SVF, CS+SVF+PRP) at 3 months post-implantation. Micro-CT scans (top row) and histological micrographs (bottom row) of the bone defect area. Histological sections stained with hematoxylin and eosin (HE); magn. ×200.
Source: Image is from authors' own archive.

Table 1: Results of clinical blood analysis in control and experimental groups.

parameter	CS		CS+SVF		CS+SVF+PRP		p-value	Units
	M	SD	M	SD	M	SD		
WBC	10.9	2.3	11.1	2.1	12.3	0.7	0.212	$\times 10^9$/L
LYM%	48.6	5.7	49.8	6.0	53.3	0.9	*p*0.119	%
MID%	21.8	2.3	20.3	2.9	21.6	1.8	0.314	%
GRAN%	29.6	6.9	30.0	7.1	25.0	1.4	0.139	%
LYM#	5.4	1.5	5.5	1.2	6.6	0.5	0.077	$\times 10^9$/L
MID#	2.4	0.7	2.3	0.5	2.7	0.1	0.205	$\times 10^9$/L
GRAN#	3.2	0.8	3.3	1.0	3.1	0.3	0.817	$\times 10^9$/L
RBC	6.1	0.3	6.0	0.2	5.8	0.2	0.053	$\times 10^{12}$/L
HGB	13.1	0.2	14.1	1.2	14.3	0.5	0.017*	g/L
HCT	38.3	1.3	36.3	1.5	37.2	1.2	0.029*	%
MCV	63.8	2.0	64.1	1.9	63.5	2.9	0.822	fL
MCH	22.9	1.3	23.6	1.5	22.2	0.9	0.089	pg
MCHC	36.3	1.0	36.8	0.7	36.0	1.3	0.236	g/L
RDW-SD	35.6	3.4	33.6	2.4	34.9	4.2	0.403	fL
RDW-CV	15.9	1.2	15.2	1.3	15.6	1.9	0.551	%
PLT	342.7	81.8	400.8	100.8	437.7	60.0	0.077	$\times 10^9$/L
MPV	7.0	0.3	7.1	0.4	7.1	0.2	0.678	fL
PDW	8.1	0.7	8.5	0.8	7.4	0.5	0.019*	i.u.
PCT	0.3	0.1	0.3	0.0	0.4	0.0	0.007*	%
P-LCR	5.1	3.4	5.5	2.1	7.4	3.1	0.200	%

Statistically significant differences compared to the CS group (*), $p \leq 0.05$.

Table 2: Micro-CT results: tissue volume and surface area within the defect zone, and surface density of the material in control and experimental animal groups.

quantification	CS M±SD	CS+SVF M±SD	CS+SVF+PRP M±SD
tissue volume, mm^3	7.62 ± 0.34	12.85 ± 0.55*	18.24 ± 0.72*#
surface area, mm^2	108.02 ± 5.19	269.83 ± 12.27*	309.25 ± 14.51*#
surface density, mm^2/mm^3	14.97 ± 0.69	15.81 ± 0.68	16.72 ± 2.53*

Statistically significant differences compared to the CS group (*) and CS+SVF+PRP vs CS+SVF (#), $p \leq 0.05$.

Table 3: Semi-quantitative scoring of morphological parameters in the implantation area in control and experimental groups.

Morphology	CS	CS+SVF	CS+SVF+PRP
Implant resorption	1	2	3
Bone tissue formation	1	2	3
Proliferative inflammation	2	1	1
Exudative inflammation	1	0	0
Neovascularisation	1	1	2
Fibrosis	0	0	0
Necrosis	0	0	0

4 Discussion

This study focuses on the significant evaluation of osteohistogenesis and neoangiogenesis stimulated by platelet-rich plasma (PRP) in combination with stromal vascular fraction (SVF) cells on a collagen matrix scaffold.

Micro-computed tomography revealed effective scaffold osteointegration and inward growth of bone trabeculae into the implantation site in all groups, with the most prominent changes observed in the CS+SVF+PRP group. Morphological assessment confirmed that the combination of SVF and PRP significantly enhanced both osteohistogenesis and neovascularisation in the critical-size bone defect area. In the control group, replacement of the biodegradable scaffold with bone tissue accounted for approximately 25% of the defect volume. It consisted of isolated reticulated-trabecular structures with osteogenic cells, primarily osteoclasts. In the SVF and SVF+PRP groups, scaffold resorption reached one-third and two-fifths of the defect area, respectively. These groups demonstrated more active bone formation—moderate and pronounced osteogenesis—and enhanced vascularisation, particularly in the CS+SVF+PRP group, where the number of newly formed vessels was the highest. This effect is likely associated with the action of growth factors contained in PRP, particularly vascular endothelial growth factor (VEGF), whose pro-angiogenic properties have been well documented (16,17). Furthermore, the absence of fibrosis and necrosis in the implantation zones across all groups confirms the high biocompatibility of the scaffold components and the absence of cytotoxic effects (18).

Haematological findings, along with histological data, indicate a systemic enhancement of regenerative processes without a marked inflammatory response following implantation of the composite scaffold CS+SVF+PRP, especially in the region of the critical-size bone defect. Notably, elevated levels of hemoglobin, hematocrit, and plateletcrit were observed in this group compared to Groups I and II, which may reflect increased erythropoietic activity and activation of the platelet response associated with tissue repair and neovascularization (19,20). The observed increase in platelet count and plateletcrit in the CS+SVF+PRP group may also result from the intense release of growth factors stored in platelet α-granules, such as IGF-1, PDGF, VEGF, and TGF-β. In conjunction with the osteogenic and angiogenic potential of SVF cells, these factors likely contribute to enhanced bone regeneration and vascularization, consistent with findings reported by other authors (21-23).

Notably, total leukocyte counts, leukocyte differentials, and absolute numbers of leukocyte subpopulations remained within reference ranges across all groups, suggesting the absence of a systemic inflammatory response. However, histological evaluation revealed differences in local inflammatory reactions. In the control group, a moderate inflammatory response characterized by mononuclear lymphohistiocytic infiltration was observed in the peri-implant area. In contrast, in the experimental groups—and especially in the CS+SVF+PRP group—the inflammatory response was minimal, with only a few isolated immune cells present. This likely reflects the immunomodulatory and anti-inflammatory properties of both SVF cells and the bioactive components of PRP (24-26).

The limitations of this study include the small sample size, the lack of histochemical differentiation of the structures of newly formed bone tissue, and the short duration of the experimental study, as well as immunophenotyping of SVF cells and molecular genetic analysis of specific participants in regulatory signaling pathways involved in osteogenesis and neoangiogenesis.

5 Conclusion

The present study demonstrates the high biocompatibility of all components of the first developed multicomponent scaffold, which includes a collagen matrix, stromal vascular fraction, and platelet-rich plasma. Their combined application produced a pronounced synergistic effect, contributing to the activation of osteohistogenesis and neoangiogenesis, as confirmed by

micro-CT and histological analysis: an increase in the volume of connective tissue and the density of newly formed bone in combination with a high level of bioresorption and the absence of peri-implant inflammation. This combination appears to be a promising approach for use in regenerative medicine and tissue engineering for the treatment of critical-size bone defects.

Conflict of Interest

None declared.

References

1. Steppe L, Megafu M, Tschaffon-Müller ME, Ignatius A, Haffner-Luntzer M. Fracture healing research: recent insights. Bone Rep. 2023;19. DOI: 10.1016/j.bonr.2023.101686 PMID: 38163010
2. Zhang LY, Bi Q, Zhao C, Chen JY, Cai MH, Chen XY. Recent advances in biomaterials for the treatment of bone defects. Organogenesis. 2020;16(4):113-25. DOI: 10.1080/15476278.2020.1808428 PMID: 32799735
3. Schemitsch EH. Size Matters: Defining Critical in Bone Defect Size! J Orthop Trauma. 2017;31:S20-2. DOI: 10.1097/BOT.0000000000000978 PMID: 28938386
4. Richter RF, Vater C, Korn M, Ahlfeld T, Rauner M, Pradel W, et al. Treatment of critical bone defects using calcium phosphate cement and mesoporous bioactive glass providing spatiotemporal drug delivery. Bioact Mater. 2023;28:402-19. DOI: 10.1016/j.bioactmat.2023.06.001 PMID: 37361564
5. Culla AC, Vater C, Tian X, Bolte J, Ahlfeld T, Bretschneider H. Treatment of critical size femoral bone defects with biomimetic hybrid scaffolds of 3D plotted calcium phosphate cement and mineralized collagen matrix. Int J Mol Sci. 2022;23(6):3400. DOI: 10.3390/ijms23063400 PMID: 35328820
6. Shcherbakov IM, Klimashina ES, Evdokimov PV, Tikhonov AA, Putlayev VI, Shipunov GA, et al. Properties of calcium phosphate/hydrogel bone grafting composite on the model of diaphyseal rat femur's defect: experimental study. Traumatology and Orthopedics of Russia. 2023;29(1):25-35. DOI: 10.17816/2311-2905-2039 PMID: 27497695
7. Chen D, Liu S, Chu X, Reiter J, Gao H, McGuire P, et al. Osteogenic differentiation potential of mesenchymal stem cells using single cell multiomic analysis. Genes (Basel). 2023;14(10):1871. DOI: 10.3390/genes14101871 PMID: 37895219
8. Pourlak T, Pourlak T, Ghodrati M, Mortazavi A, Dolati S, Yousefi M. Usage of stem cells in oral and maxillofacial region. J Stomatol Oral Maxillofac Surg. 2021;122(4):441-52. DOI: 10.1016/j.jormas.2020.10.003 PMID: 33099018
9. Łuczak JW, Palusińska M, Matak D, Pietrzak D, Nakielski P, Lewicki S, et al. The future of bone repair: emerging technologies and biomaterials in bone regeneration. Int J Mol Sci. 2024;25(23):12766. DOI: 10.3390/ijms252312766 PMID: 39684476
10. Garimella A, Ghosh SB, Bandyopadhyay-Ghosh S. Biomaterials for bone tissue engineering: Achievements to date and future directions. Biomed Mater. 2024;20(1). DOI: 10.1088/1748-605X/ad967c PMID: 39577395
11. Dewey MJ, Milner DJ, Weisgerber D, Flanagan CL, Rubessa M, Lotti S, et al. Repair of critical-size porcine craniofacial bone defects using a collagen-polycaprolactone composite biomaterial. Biofabrication. 2021;14(1):303-10. PMID: 34663761
12. Goncharov EN, Koval OA, Bezuglov EN. Comparative analysis of stromal vascular fraction and alternative mechanisms in bone fracture stimulation: A systematic review. Biomedicines. 2024;12(2):342.
13. Sananta P, Oka IG, Dradjat PR. Adipose-derived stromal vascular fraction prevents bone bridge formation on growth plate injury in rats: an in vivo experimental study. Ann Med Surg (Lond). 2020;60:211-7. DOI: 10.1016/j.amsu.2020.09.026 PMID: 33194176
14. Bacevich BM, Smith RD, Reihl AM, Mazzocca AD, Hutchinson ID. Advances with platelet-rich plasma for bone healing. Biologics. 2024;18:29-59. PMID: 38299120
15. Everts PA, Podesta L, Lana JF, Shapiro G, Domingues RB, van Zundert A, et al. he Regenerative Marriage Between High-Density Platelet-Rich Plasma and Adipose Tissue. Int J Mol Sci. 2025;26(5):2154. DOI: 10.3390/ijms26052154 PMID: 40076775
16. Zhang M, Fukushima Y, Nozaki K, Nakanishi H, Deng J, Wakabayashi N, et al. Enhancement of bone regeneration by coadministration of angiogenic and osteogenic factors using messenger RNA. Inflamm Regen. 2023;43(1):32. DOI: 10.1186/s41232-023-00285-3 PMID: 37340499
17. Zhang Y, Xing F, Luo R, Duan X. Platelet-rich plasma for bone fracture treatment: A systematic review of current evidence in preclinical and clinical studies. Front Med (Lausanne). 2021;8. DOI: 10.3389/fmed.2021.676033 PMID: 34414200
18. Tupe A, Patole V, Ingavle G, Kavitkar G, Mishra Tiwari R, Kapare H, et al. Recent advances in biomaterial-based scaffolds for guided bone tissue engineering: challenges and future directions. Polym Adv Technol. 2024;35(11). DOI: 10.1002/pat.6619
19. Childress PJ, Nielsen JJ, Bemenderfer TB, Dadwal UC, Chakraborty N, Harris JS, et al. Thrombopoietic agents enhance bone healing in mice, rats, and pigs. J Bone Miner Res. 2024;40(1):125-39. DOI: 10.1093/jbmr/zjae191 PMID: 39566068
20. Vasileva R, Chaprazov T, Milanova A. Effects of erythropoietin-promoted fracture healing on bone turnover markers in cats. J Funct Biomater. 2024;15(4):106. DOI: 10.3390/jfb15040106 PMID: 38667563
21. Li S, Xing F, Luo R, Liu M. Clinical effectiveness of platelet-rich plasma for long-bone delayed union and nonunion: A systematic review and meta-analysis. Front Med (Lausanne). 2022;8. DOI: 10.3389/fmed.2021.771252 PMID: 35145974
22. Ranjan R, Kumar R, Jeyaraman M, Arora A, Kumar S, Nallakumarasamy A, et al. Autologous platelet-rich plasma in the delayed union of long bone fractures - A quasi experimental study. J Orthop. 2022;36:76-81. DOI: 10.1016/j.jor.2022.12.013 PMID: 36620095
23. Van Lieshout EM, Den Hartog D. Effect of platelet-rich plasma on fracture healing. Injury. 2021;52:S58-66. DOI: 10.1016/j.injury.2020.12.005 PMID: 33431160
24. Kale P, Shrivastava S, Pundkar A, Balusani P. Harnessing healing power: A comprehensive review on platelet-rich plasma in compound fracture care. Cureus. 2024;16(1). DOI: 10.7759/cureus.52722 PMID: 38384641
25. Malcangi G, Patano A, Palmieri G. Maxillary sinus augmentation using autologous platelet concentrates (PRP, PRF, and CGF) combined with bone graft: A systematic review. Cells. 2023;12(13):1797. DOI: 10.3390/cells12131797 PMID: 37443831
26. Fang J, Wang X, Jiang W, Zhu Y, Hu Y, Zhao Y, et al. Platelet-rich plasma therapy in the treatment of diseases associated with orthopedic injuries. Tissue Eng Part B Rev. 2020;26(6):571-85. DOI: 10.1089/ten.teb.2019.0292 PMID: 32380937